Available online at www.sciencedirect.com
ScienceDirect
Catalysis Today 130 (2008) 56–62
CATALYSIS TODAY
www.elsevier.com/locate/cattod

Highly dispersed CoMoS phase on titania nanotubes as efficient HDS catalysts

M.A. Cortés-Jácome, J. Escobar, C. Angeles Chávez, E. López-Salinas, E. Romero, G. Ferrat, J.A. Toledo-Antonio *

Molecular Engineering Program, Instituto Mexicano del Petróleo, Eje Central Lázaro Cárdenas #152, San Bartolo Atepehuacan, G.A. Madero, 07730 México, D.F., Mexico

Available online 31 August 2007

Abstract

Nanotubular titania (NT) to be used as support for CoMo-based hydrodesulfurization (HDS) catalyst was synthesized and characterized by various techniques. NT annealed at 400 °C (under nitrogen) was constituted by nanotubes of ~5.5 nm (internal diameter) and retained 236 m^2/g of surface area. Mo at 3 atoms/nm^2 (nominal loading) and cobalt at Co/(Co + Mo) = 0.3 were impregnated under nearly neutral, acidic or basic media. By XPS analyses of NT-supported sulfided catalysts, highly dispersed MoS_2 particles of low stacking degree (1–2 slabs) aligned along the nanotubes were observed by HR-TEM in all sulfided materials. The CoMo catalysts supported on nanostructured titania had dibenzothiophene (DBT) HDS activity (in pseudo first order kinetic constant basis) values ~1.35 and ~1.7 times (Mo impregnated under near neutral and basic media, respectively) higher to that of a commercial reference with alumina carrier. According to shifts to higher binding energy of the Co 2p peak corresponding to sulfided cobalt (as determined by XPS), MoS_2 dispersed on NT support could be efficiently promoted by Co (''CoMoS'' phase formation), opening the possibility of developing new highly active HDS catalysts.

Keywords: HDS catalysts; Titania; CoMoS; XPS; HRTEM; Nanotubes support

1. Introduction

The more stringent environmental regulations that limit maximum sulfur content in diesel at ~10–15 wt ppm, have been the driving force for refiners to produce ultra-low sulfur fuels at affordable costs either by upgrading existing technologies or by developing new oil refining processes, including more active hydrodesulfurization (HDS) catalysts. The application of more active catalytic materials could result in improvements in fuel quality without negative impact on capital investment.

Industrially, HDS of middle distillates is carried out on sulfided either $CoMo/Al_2O_3$ or $NiMo/Al_2O_3$ catalysts. The properties of those sulfided catalysts strongly depend on the interaction of the impregnated phases with the support that in turn, could influence dispersion, sulfidability and promotion degree of MoS_2 by neighboring Co and Ni. These facts could determine the efficiency of the formation of the so called ''CoMoS'' or ''NiMoS phase'' [1,2], in which S vacancies occurring at edge/corner sites of MoS_2 crystallites are considered to be the active sites for HDS reactions. When supported on alumina, these sites were formerly classified as ''Type I'' when located in sulfided Mo exhibiting lower S coordination and high dispersion of MoS_2 slabs [3]. On the other hand, when this phase was less dispersed and fully sulfided ''Type II'' sites were present [3]. CoMoS Type II sites are reported to be more active than Type I ones [3]. Highly active CoMoS Type II sites of low stacking degree can be obtained by replacing the alumina support by other carriers, such as carbon, showing weaker interaction with the impregnated phases [3]. One of the most promising supports for HDS catalysts is titania, due to the enhanced activity that have been observed for the corresponding sulfided catalysts [4,5]. Accordingly, TiO_2 with relative high surface area (e.g. 120–160 m^2/g) has been developed with improved textural properties, the carrier being able to efficiently disperse Mo [5] or Co–Mo phases [6]. The corresponding $CoMo/TiO_2$ formulation enabled the production of ultra low sulfur diesel

* Corresponding author. Tel.: +52 55 91 75 8433.
E-mail address: jtoledo@imp.mx (J.A. Toledo-Antonio).

0920-5861/$ – see front matter
doi:10.1016/j.cattod.2007.07.012

(ULSD) of ~10 ppm S at operating conditions at which over an alumina supported commercial reference a S content of about 200 ppm was observed in the diesel product. Recently, we synthesized high surface area (>300 m^2/g) nanotubular titania (NT) where the supported CoMoS phase was both highly dispersed and highly sulfided, these characteristics being reflected in enhanced activity in DBT HDS [7]. In the present contribution, the effect of the pH of the impregnating solution on the CoMoS phase dispersion was studied in materials at 3 Mo at./nm^2 nominal loading on the NT support.

2. Experimental

2.1. Synthesis of support

NT support was synthesized by a hydrothermal method as described in [8], starting from a TiO_2 anatase (Hombitec K03, provided by Sachtleben Chemie). TiO_2 anatase powder was suspended in an aqueous 10 M NaOH solution and the resulting suspension was placed in an autoclave at 100 °C for 24 h under stirring. Thereafter, the white slurry was filtered and neutralized with 1 M HNO_3 overnight. Then, the material was washed and dried at 110 °C yielding a hydrous titania powder with nanotubular morphology.

2.2. Catalysts preparation

CoMo-based catalysts were prepared from high surface area NT by impregnation at incipient wetness. For all materials, the nominal Mo loading was 3 atoms/nm^2 taking into account the surface area of the dried support (369 m^2/g) meanwhile cobalt was added at Co/(Co + Mo = 0.3). In the first case, the carrier was contacted with aqueous ammonium heptamolybdate (AHM) solutions at natural pH (5.6, close to neutral, ''N''). After drying at 120 °C, cobalt was deposited on the Mo-containing samples through a $(CH_3CO_2)_2Co{\cdot}4H_2O$ solution. Another sample was prepared by Mo impregnation under basic (''B'') conditions at pH 10.0, by addition of some drops of NH_4OH (28 vol.%) to the original AHM solution. In this case, Co was deposited following the procedure already mentioned for the previous formulation. Finally, a third sample was impregnated under acidic (''A'') conditions in one step. The impregnating solution was prepared by digesting MoO_3 with cobalt acetate and phosphoric acid at 95 °C (all of them in aqueous solution). The final acidic solution had a pH ~1.8. For all impregnated materials, further processing included drying at 120 °C and annealing at 380 °C under air flow. Hereinafter the catalysts will be referred to as NTB-3, NTN-3 and NTA-3 where NT stands for the nanotubular support; B, N and A represents the conditions of Mo impregnation and the number 3 indicates the nominal amount of Mo atoms per nm^2. Catalysts sulfidation was carried out over oxidized samples under H_2S/H_2 10 vol.%. First, the solids were brought to 380 °C, under N_2 atmosphere (100 mL/min), and then the gas flow was switched to an in situ made H_2S/H_2 mixture (6/50 mL/min). These conditions were maintained during 1 h.

2.3. Catalysts evaluation

Sulfided catalysts (~0.2 g) were tested in HDS of model molecule (DBT, ~0.3 g) in a batch reactor using *n*-hexadecane as solvent (100 mL). The reaction conditions were 320 °C, 1000 rpm and 56 kg/cm^2 and sulfided catalysts were used as particles of 80–100 U.S. standard mesh size (~0.165 mm average particle diameter). These conditions were carefully chosen to avoid reaction control by internal/external diffusion phenomena. Liquid products were analyzed in a Varian 3400 CX gas chromatograph (FID detector and dimethylpolysiloxane capillary column, 50 m × 0.2 mm × 0.5 μm). HDS kinetic constants were calculated assuming pseudo-first order kinetics referred to DBT concentration (x = conversion, t = time):

$$k = \frac{-\ln(1-x)}{t}$$

2.4. Catalysts characterization

Textural properties of various materials were determined by N_2 physisorption (at −196 °C), in a Micromeritics ASAP 2000 apparatus. Chemical composition of the impregnated materials after annealing at 380 °C was determined by atomic absorption spectroscopy (AAS) with a Perkin-Elmer 2380 apparatus. Identities of crystalline phases in the annealed and sulfided materials were examined by X-ray diffraction. Patterns of the samples ($5 < 2\theta < 70^\circ$) packed in a glass holder were recorded at room temperature with $Cu_{K\alpha}$ radiation (λ = 1.5406 Å) in a Siemens D-500 diffractometer with a graphite secondary beam monochromator. The $Cu_{K\alpha 1}$ contribution was eliminated by DIFFRAC/AT software. Raman spectra were recorded at room temperature using a Jobin Yvon Inc. Horiba T64000 spectrometer, equipped with a confocal microscope (Olympus, BX41) with a laser beam (514.5 nm) at a power level of 3 mW. Sulfided catalysts were also analyzed by X-ray photoelectronic spectroscopy (XPS). The corresponding spectra were obtained in a THERMO-VG SCALAB 250 spectrometer equipped with $Al_{K\alpha}$ X-ray source (1486.6 eV) and a hemispherical analyzer. Experimental peaks were decomposed into components using mixed Gaussian–Lorentzian functions and a non-linear squares fitting algorithm. Shirley background subtraction was applied. Binding energies were reproducible within ±0.2 eV and the C 1s peak (from adventitious carbon) at 284.6 eV was used as a reference. Surface elemental composition was determined by fitting and integrating the Co 2p, Mo 3d, S 2p, C 1s, O 1s and Ti 2p bands and converting these values to atomic ratios using theoretical sensitivity factors provided by the manufacturer of the XPS apparatus [9]. The sulfided catalysts were kept under inert atmosphere by using a glove box and a special box vessel to introduce the samples into the spectrometer analysis chamber. High-resolution transmission electron microscopy (HR-TEM) analysis of the samples was performed in a JEOL 2010F microscope operating at 200 kV, and equipped with a Schottky-type field emission gun and an ultrahigh resolution pole piece (Cs = 0.5 mm; point to point resolution, 0.190 nm). The support and sulfided catalysts were ground, suspended in

Table 1
Chemical composition (as determined by AAS) of calcined catalysts

Sample	Mo (wt.%)	Co (wt.%)	Co/(Co + Mo) atomic ratio
NTB-3	12.51	3.14	0.29
NTN-3	12.83	3.13	0.28
NTA-3	11.78	3.19	0.31
PCoMo/Al_2O_3	14.60	3.50	0.29

isopropanol at room temperature, and finally dispersed by ultrasonic agitation. Then, the corresponding suspensions were dropped on a 3 mm diameter lacey carbon copper grid.

3. Results and discussion

Chemical composition of the calcined catalysts (determined by AAS) is shown in Table 1. Actual Mo and Co concentrations were quite similar to the nominal ones, maintaining the Co/(Co + Mo) atomic ratio close to 0.3. For sake of comparison, chemical composition of the commercial alumina-supported catalyst used as reference is included, showing quite similar Co/(Co + Mo) atomic ratio as to those prepared over titania nanotubes.

Textural properties of the support and calcined impregnated samples are presented in Table 2. Initially, NT dried support showed a high surface area (SSA) of 369 m^2/g, with average pore diameter of 6.3 nm. After calcining at 400 °C, its SSA was 236 m^2/g. Impregnation and further annealing resulted in materials where SSA and pore volume slightly decreased, as compared with the support, as consequence of the impregnation of non-porous CoMo phase [10] and also by structural changes that the nanostructured support underwent during annealing treatment [11]. As a reference, the textural properties of a PCoMo alumina supported commercial catalysts are included in Table 2.

X-ray diffraction (XRD) patterns of the calcined support and impregnated materials after annealing and final catalysts are shown in Fig. 1a and b, respectively. All of them show three main peaks at 24.5, 28.0, 48.5° in 2θ position that have been previously assigned to the orthorhombic phase of layered titanates [12,13]. The presence of anatase peaks was not evident even after annealing at 400 °C, suggesting that nanotubular structure remain stable in the support and after impregnation of supported phases. XRD of sulfided catalysts showed same crystallographic phases as those observed in the corresponding oxidized phases (Fig. 1b). No evidence of any sulfided or oxidized segregated phases was observed, suggesting highly-dispersed deposited species on the support.

Table 2
Textural properties of support (after drying and annealing) and catalysts after calcination

Samples	Specific surface area (m^2/g)	Total pore volume (cm^3/g)	Average pore size (nm)
NT	369	0.58	6.3
NT-400°C	236	0.52	6.8
NTB-3	216	0.46	7.0
NTN-3	229	0.45	6.6
NTA-3	204	0.39	7.3
PCoMo/Al_2O_3	225	0.50	8.9

Raman spectra of the calcined support and impregnated precursors after annealing are shown in Fig. 2. The bands of anatase were evident on the support by the band at 144 cm^{-1} corresponding to the E*g* vibration [14]. Other bands corresponding to anatase phase at 200, 400, 505, 640 and 796 cm^{-1} were less intense and broadened in impregnated samples. Reflections corresponding to the nanotubular structure were observed at 280, 450 and 700 cm^{-1} [15]. Then, after calcination the structure of the NT support is composed by a mixture of anatase and orthorhombic layered phases, suggesting the formation of anatase domains in some regions of the nanotubes walls [16]. CoMo impregnation on nanotubes stabilizes the orthorhombic structure of titania against its

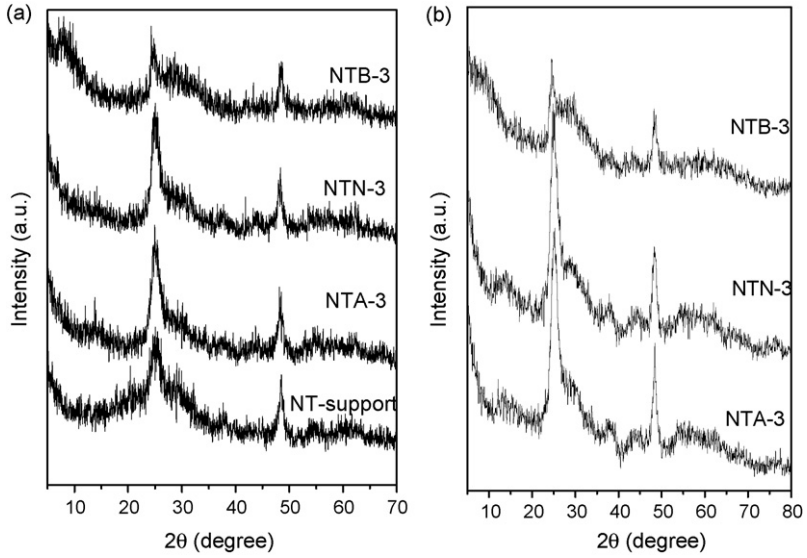

Fig. 1. XRD patterns of nanostructured (NT) carrier and CoMo/NT: (a) annealed in N_2 atmosphere and (b) sulfided samples.

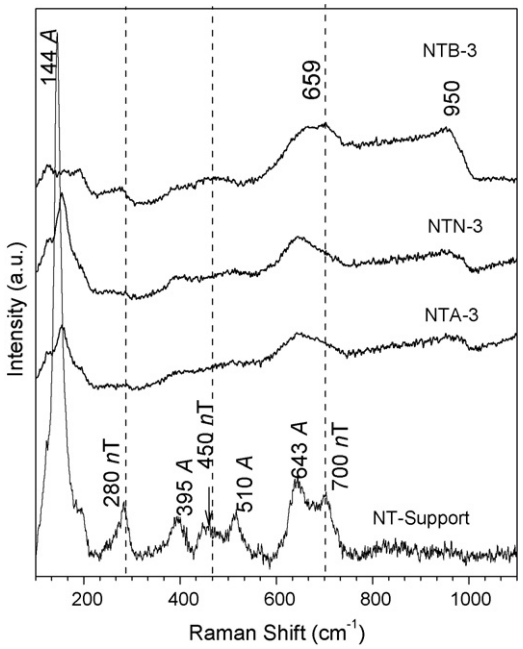

Fig. 2. Raman spectra of calcined NT support and oxidized CoMo supported on NT impregnated at different pH.

transformation into anatase, since the vibrating band corresponding to E*g* of anatase became broad and shifted to higher frequencies for impregnated NTA and NTN samples and it practically disappeared in NTB sample. Compared with NT support, after annealing at 400 °C, all the vibrating bands of anatase phase were evident. Then, Co and Mo impregnation inhibit the transformation of nanotubular support from orthorhombic to tetragonal anatase phase.

Regarding the CoMo phase deposited on NT support, a broad band arising from 800 to 970 cm^{-1} was observed, independently of the pH of impregnation. This band corresponds to the asymmetrical vibration of terminal Mo=O O bonds [17]. The intensity of the broad band around 660 cm^{-1} increased considerably compared with the bands at 278 and 450 cm^{-1}, then, the major contribution to the band around 660–700 cm^{-1} comes from the oxidized CoMo phase, suggesting that the structure is the β-$CoMoO_4$ phase [18,19]. For the PCoMo/Al_2O_3 commercial catalyst, only a broad band centered at 954 cm^{-1} was previously observed [18], which has been assigned to terminal Mo=O stretching modes in octahedral environment.

TEM images of the support showed mainly material with nanotubular morphology (Fig. 3a). The internal diameter of nanotubes is ca. 5.5 nm, which roughly correspond to the pore size diameter (Table 2). After CoMoS phase impregnation in NTN-3 sample, Fig. 3b, nanotubular morphology remained unchanged. At high magnification in Fig. 3c and d, the structure of MoS_2 can be detected as well-dispersed crystallites of low staking degree (one or two layers) located in between the nanotubes of the support. Particularly, in Fig. 3d it can be observed that the structural layers of MoS_2 (mainly two staked layers) grew along the nanotubes direction (arrows in Fig. 3d) with an interlayer spacing of 0.61 nm [3].

From these images it can be concluded that NT are suitable as support for highly-dispersed CoMoS phase, as it was corroborated in the following XPS studies.

Surface elemental composition determined by XPS showed that Co and Mo atoms are well dispersed on NT, regardless the impregnation pH (Table 3). However, it should be noted that neither all dispersed Co and Mo atoms were sulfided upon the H_2S/H_2 treatment at high temperature nor all the sulfided Co atoms are promoting the MoS_2 phase forming the so called ''CoMoS'' phase [1,2]. To determine Co and Mo sulfided species, the Co 2p and Mo 3d XPS spectra were fitted and integrated as shown in Fig. 4, for NTB-3 sample. Mo 3d doublet was well-fitted by considering Mo^{4+} from totally sulfided MoS_2, Mo^{5+} from molybdenum oxy-sulfides and Mo^{6+} from unreduced molybdenum oxide [20] (see Fig. 4a). Meanwhile, Co 2p spectra were fitted with three doublets (Fig. 4b), the first one at 779.0–779.5, from sulfided Co–S, the second one at 781.5–781.9 from oxidized Co–O, and the third one, from a broadened peak satellite signal [21,22]. For NT-supported samples, the amount of CoS decreased from 1.48 to 0.47 at.% with the impregnation pH. However, sulfided Mo^{4+} was better dispersed on NT at neutral than at basic or acid impregnation pH, Table 3. Mo $3d_{5/2}$ binding energy (BE) registered for sulfided Mo^{4+} species remained close at 229.0 ± 0.2 eV for all the samples (Table 4) corresponding to BE value reported for MoS_2 phase by others [20]. The Co $2p_{3/2}$ BE was 779.0 eV for the sample where Mo was impregnated under acidic conditions and shifted to 779.3 eV in catalysts prepared at higher pH. According to other authors [21,23], the BE value reported for segregated Co_9S_8 phase is around 778.5 eV. Even more, when Co species chemically interact with the edge sites of MoS_2 particles (to form the ''CoMoS'' phase), the BE shifts to a value ∼0.9 eV higher than that for Co_9S_8. Then, the results shown in

Table 3
Surface atomic chemical composition (as determined by XPS) of sulfided catalysts

Samples	Surface chemical composition (at.%)									
	S	Ti	Al	Co_{tot}	Co–S[a]	Co–O[b]	Mo_{tot}	Mo^{4+}	Mo^{5+}	Mo^{6+}
NTB-3	8.94	29.6	0	2.47	1.48	0.99	6.86	4.83	1.66	0.37
NTN-3	17.8	27.9	0	2.83	1.34	1.49	8.7	5.79	1.38	1.53
NTA-3	5.09	32.3	0	1.9	0.47	1.43	6.17	3.42	2.11	0.64
PCoMo/Al_2O_3	5.16	0	34.7	1.09	0.18	0.91	5.26	2.86	0.96	1.44

[a] Sulfided Co.
[b] Oxidized Co.

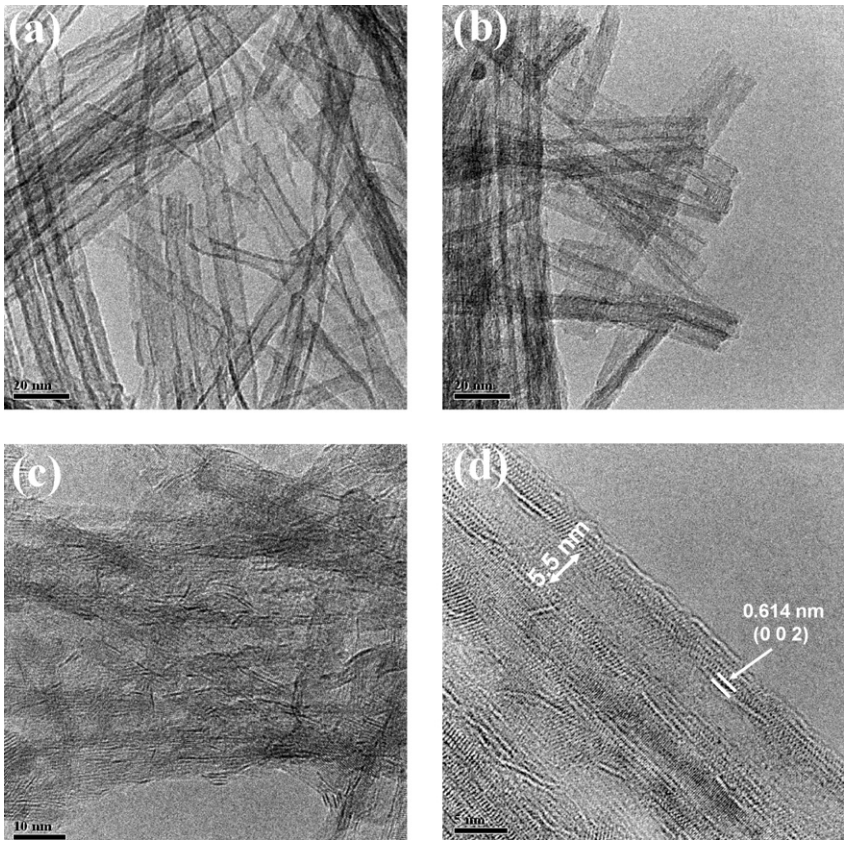

Fig. 3. TEM images of (a) NT support and (b) NTN-3 impregnated and (c) sulfided catalyst. In (d), HRTEM images of isolated nanotubes with MoS_2 slabs.

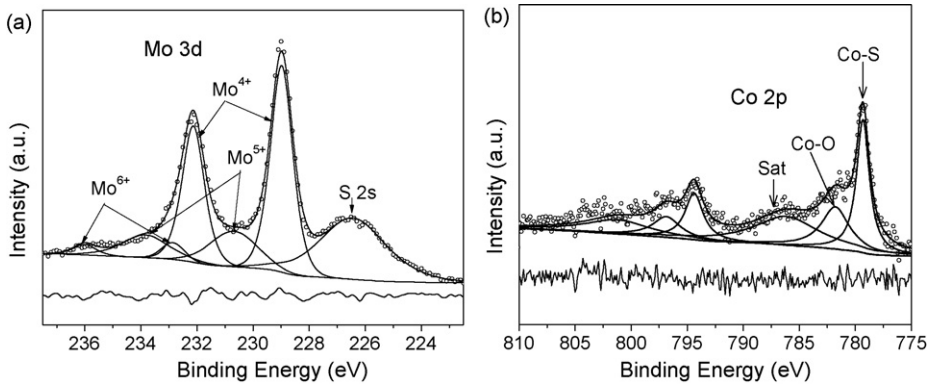

Fig. 4. Representative XPS of: (a) Mo 3d spectrum, and (b) Co 2p spectrum, both from NTN-3 sample. Co satellite signal is indicated as ''Sat''.

Table 4
Binding energy at FWHM values of atomic components on sulfided catalysts

Samples	Binding energy FWHM (eV)			
	S (2p)	Ti $(2p)_{3/2}$	Co $(2p)_{3/2}$[a]	Mo $(3d)_{5/2}$[b]
NTB-3	161.7	459.2	779.3	229.0
NTN-3	161.2	458.9	779.3	228.6
NTA-3	161.8	459.3	779.0	229.0
$PCoMo/Al_2O_3$	161.7	–	779.8	229.0

[a] Sulfided Co.
[b] Sulfided Mo.

Table 4 strongly suggest that Co species introduced on Mo species impregnated at basic and neutral pH give rise (in the final catalyst) to sulfided species in closer interaction with MoS_2 particles, than those obtained by sulfiding Co–Mo simultaneously impregnated at acid pH. Based on these facts, it can be assumed that higher amounts of ''CoMoS'' phase are produced when Mo has been deposited at natural or basic pH. Then, in the NTB-3 and NTA-3 sulfided catalysts good promotion of MoS_2 by Co could be expected. This fact would be reflected in enhanced HDS activity. In the opposite of that we found, it has been reported that in titania-supported catalyst promotion of MoS_2 by Co is rather poor [24,25]. However, it

Table 5
Pseudo-first order kinetic constant (DBT HDS) on various sulfided CoMo catalysts supported on nanostructured titania and alumina

Sample	$k \times 10^5$ (m^3/kg_{cat} s)	$k' \times 10^{-5}$ (m^3/kg_{Mo} s)
NTB-3	15.8	126.3
NTN-3	20.0	155.9
NTA-3	5.5	46.7
PCoMo/Al_2O_3	11.7	80.1

Batch reactor, 320 °C, 56 kg/cm^2, 1000 rpm mixing speed, *n*-hexadecane as solvent.

should be noted that in most of the cases anatase titania was used as catalyst carrier. It seemed that distinctive properties of our nanostructured support could play a major role in obtaining materials were ''CoMoS'' phase formation appeared to be enhanced.

Comparatively, an alumina-based catalyst was used as reference, and NT-catalysts showed higher Co and Mo dispersion, regardless of the impregnation pH (Table 3). It is important to remark that the reference was a conventional commercial catalyst sulfided by using exactly the same procedure as in our catalysts where NT was used as carrier (see Section 2.2). For the CoMoP/Al_2O_3 catalyst, we attempted different methodologies to try to assess the effect of that preparation step on the Mo and Co sulfiding degree obtained (e.g. (i) admitting H_2S/H_2 at room temperature and then increasing the temperature to 380 °C, (ii) oxidizing first in air at 380 °C and then admitting H_2S/H_2, (iii) first annealing in nitrogen at 380 °C and then admitting H_2S/H_2). We found that CoMoP/Al_2O_3 sulfidation was essentially not affected by variations in the activation procedure used. As can be observed from Table 3 data, Co dispersion was considerably higher in NT-catalysts than that in alumina, suggesting that a large amount of Co atoms react with Al_2O_3 carrier yielding $CoAl_2O_4$ surface species which are difficult to sulfide. Conversely, in our NT-supported samples, all Co atoms appeared to react with Mo atoms to produce $CoMoO_4$ surface species, in which a larger population of Co atoms is easier to sulfide.

As observed in Table 5, the DBT HDS activity of CoMoS supported on NT showed a maximum value at neutral pH 5.6 of Mo impregnation. Lower HDS activity was shown for the sample where Mo was impregnated at acid pH (NTA-3). This sample showed lower Co–S and sulfided Mo^{4+} concentration (see Table 4), than that impregnated at basic or neutral pH. In fact, a direct correlation can be established between the CoS and sulfided Mo^{4+} determined by XPS and the DBT HDS activity, suggesting that higher dispersion in CoS and MoS_2 correspond to higher HDS activity. Moreover, as aforementioned, the BE of Co–S in NTA-3 (Table 4) occurred at 779.0 eV suggesting that most of the Co atoms are not in close interaction with MoS_2. Thus, in this case the formation of the ''CoMoS'' could be limited. Meanwhile, in the other samples (NTB-3 and NTN-3) the Co–S BE shifted to 779.3 eV suggesting a more efficiently promoted MoS_2 phase, this fact being well-correlated with their enhanced HDS activity. In comparison to the conventional alumina-supported catalyst, the DBT HDS pseudo first order kinetic constant determined for NTN-3 was about 1.7 times higher. This improvement was even more remarkable in intrinsic pseudo kinetic constant (k') basis.

The particular topography and morphology of NT, e.g. curved surfaces, abundant tube-mouth edges, as well as the weak interaction between CoMo species and the nanostructured support, are very likely at the origin of the enhanced performance of the CoMo/NT HDS catalysts.

4. Conclusions

Nanotubular titania is a very efficient new support to disperse CoMo species which, after sulfiding, result in very active catalyst for HDS of DBT. CoMo/NT at 3 Mo atoms/nm^2 (nominal loading) and Co/(Co + Mo) = 0.3, prepared by successive impregnation (Mo deposited at pH 5.6), was twice as active (after proper sulfiding) than a commercial alumina-supported catalyst with similar CoMo loading. High concentration of Mo^{4+} and Co–S species and good MoS_2 phase promotion by Co appeared to be responsible for this behavior. In the opposite to that generally reported for HDS catalysts on titania anatase carrier, shifts to higher binding energy (as determined by XPS) of the Co 2p peak corresponding to sulfided cobalt suggested that MoS_2 dispersed on NT support could be efficiently promoted by Co, opening the possibility of developing new highly active HDS catalysts.

Acknowledgements

This work was financially supported by IMP projects D.00237, D.00446, and D.00447.

References

[1] H. Topsøe, B.S. Clausen, F.E. Massoth, in: J.R. Anderson, M. Boudart (Eds.), Catalysis Science and Technology, vol. 11, Springer, Berlin, 1996.
[2] H. Topsøe, B.S. Clausen, Catal. Rev. Sci. Eng. 26 (1984) 395.
[3] S.M.A.M. Bouwens, F.B.M. van Zon, M.P. van Dijk, A.M. van der Kraan, V.H.J. de Beer, J.A.R. van Veen, D.C. Koningsberger, J. Catal. 146 (1994) 375.
[4] K.Y.S. Ng, E. Gulari, J. Catal. 92 (1985) 340.
[5] S. Dzwigaj, C. Louis, M. Breysse, M. Cattenot, V. Bellière, C. Geantet, M. Vrinat, P. Blanchard, E. Payen, S. Inoue, H. Kudo, Y. Yoshimura, Appl. Catal. B 41 (2003) 181.
[6] S. Inoue, A. Muto, H. Kudou, T. Ono, Appl. Catal. A 269 (2004) 7.
[7] J. Escobar, J.A. Toledo, M.A. Cortés, M.L. Mosqueira, V. Pérez, G. Ferrat, E. López-Salinas, E. Torres-García, Catal. Today 106 (2005) 222.
[8] J.A. Toledo, C. Angeles Chavez, M. A. Cortés, F. Alvarez, Y. Ruiz, G. Ferrat, L.F. Flores, E. Lopez, M. Lozada, Patent WO2005105674 (2005).
[9] Thermo VG-Scientific. XPS and Auger Handbook. Doc. Number: 600001, issue 2, 2003.
[10] J. Ramirez, L. Ruiz-Ramirez, L. Cedeno, V. Harle, M. Vrinat, M. Breysse, Appl. Catal. A 93 (1993) 163.
[11] M.A. Cortés-Jácome, G. Ferrat-Torres, L.F. Flores Ortiz, C. Angeles-Chávez, E. López-Salinas, J. Escobar, M.L. Mosqueira, J.A. Toledo-Antonio, Catal. Today 126 (2007) 248.
[12] J. Yang, Z. Jin, X. Wang, W. Li, J. Zhang, S. Zhang, X. Guo, Z. Zhang, Dalton Trans. (2003) 3898.
[13] M. Sugita, M. Tsuji, M. Abe, Bull. Chem. Soc. Jpn. 63 (1990) 1978.
[14] I.R. Beattie, T.R. Gilson, Proc. Roy. Soc. A 307 (1968) 407.
[15] A. Kukovecz, M. Hodos, Z. Konya, I. Kiricsi, Chem. Phys. Lett. 411 (2005) 445.

[16] J.A. Toledo Antonio, S. Capula, M.A. Cortés-Jácome, C. Angeles Chávez, E. López Salinas, J. Navarrete, J. Escobar. J. Phys. Chem. C 111 (2007) 10799.
[17] Z.B. Wel, W. Yan, H. Zhang, T. Ren, Q. Xin, L. Zhongcheng, Appl. Catal. A 167 (1998) 39.
[18] F. Dumeignil, K. Sato, M. Imamura, N. Matsubayashi, E. Payen, H. Shimada, Appl. Catal. A 315 (2006) 18.
[19] E. Payen, S. Kasztelan, Trends Phys. Chem. 4 (1994) 363.
[20] J.C. Muijsers, Th. Weber, R.M. van Hardeveld, H.W. Zandbergen, J.W. Niemantsverdriet, J. Catal. 157 (1995) 698.
[21] I. Alstrup, I. Chorkendorff, R. Candia, B.S. Clausen, H. Topsøe, J. Catal. 77 (1982) 397.
[22] A.F.H. Sanders, A.M. de Jong, V.H.J. de Beer, J.A.R. van Veen, J.W. Niemantsverdriet, Appl. Surf. Sci. 144 (1999) 380.
[23] Y. Okamoto, T. Kubota, Catal. Today 86 (2003) 31.
[24] D. Wang, X. Li, E.W. Qian, A. Ishihara, T. Kabe, Appl. Catal. A 238 (2003) 109.
[25] J. Ramírez, S. Fuentes, G. Díaz, M. Vrinat, M. Breysse, M. Lacroix, Appl. Catal. 52 (1989) 211.